A SOURCE WAKE MODEL FOR CASCADES OF AXIAL FLOW TURBOMACHINES

Ramiro G. Ramirez Camacho.
Instituto Tecnológico de Aeronáutica CTA-ITA-IEM/IEME,
1228-900, São Jose dos Campos- SP- Brasil
rgramirez65@hotmail.com

Nelson Manzanares Filho
Universidade Federal de Itajubá UNIFEI
37500-000- Itajubá –MG-Brasil
nelson@iem.efei.br

Abstract

This work presents a computational model for the viscous flow through rectilinear cascades of axial turbomachinery. The model is based on modifications of the classical Hess & Smith panel method. The viscous effect of the attached flow portion is introduced by means of normal transpiration velocities obtained from the boundary layer calculations on the airfoil contour. At the separated flow portion, fictitious velocities semi-empirical normal velocities are introduced assuming a constant pressure in the wake. When the separation is not detected, it is possible to simulate the effect of the small wake near the trailing edge by using an injected flow on a distance based on the Gostelow (1975) fairing-in procedure. The numerical model presents two iteration cycles: the first one to find the separation point, and the second one to accomplish the viscous-inviscid interaction, in which the transpiration velocities and the flow injection are submitted to a relaxation process in order to guarantee the convergence of the method. Results for the pressure distributions, flow turning angles and lift coefficients are compared with experimental data for the model validation.

Keywords: Method of the panels, separation of boundary layer, linear cascades, interaction inviscid - viscous

Introduction

In the design of turbomachinery cascades it is often necessary to define some basic parameters such as the flow turning angle and the lift coefficient of the blade. These parameters must be high enough to guarantee the highest pressure rise through the machine without compromising its efficiency with aerodynamic loadings typical of stall. The result is that axial flow turbomachines usually operate at nominal conditions with significant areas of boundary layer separation. This fact has been observed by some researchers such as Lieblein (1959) and Schlichting (1959), and has been confirmed theoretically by boundary layer analysis and experimentally in tunnels of cascades and axial compressor rig. Therefore situations of flow separation must be necessarily considered in the preliminary design.

The determination of the fluid in turbo machines many works, based on singularities distribution techniques, have been reported for potential fluid field determination in isolated or cascaded airfoils, where viscous effects are quantified through transpiration normal velocities obtained from developed boundary layer (Lighthill, 1958), known as "inviscid/viscous interaction". These techniques offer satisfactory results, especially in situations where boundary layer separation hasn't been detected in the proximity of the trailing edge, like in Bizarro and Girardi's work, (1998) based on the Hess and Smith (1996) potencial model produce technique.

Works based on coupled inviscid-viscous interaction, where the potential model is determined through singularity distributions around airfoils and integral methods of boundary layer to determine the viscous effect, have the vantage of less computational effort compared to full Navier-Stokes solution models as showed previously. The potential model based on boundary elements such as the panel's technique is more appropriate for inviscid flow calculation because it doesn't require iteration and can be considered as fully accurate at each stage and consequently it requires less computational effort compared to other methods.

Considering these aspects, the use of alternative methods with low computational cost can be attractive in the turbomachinery preliminary design. Ramirez and Manzanares (2000) have proposed a model for the simulation of boundary layer separation in cascades of turbomachinery based on the Hess and Smith (1967) panel technique. The classical impenetrability condition on the blade surface was modified by flow injection in the area of separation, according to the empirical procedure by Hayashi & Endo (1977). In the situation there is no boundary layer separation, transpiration velocities are introduced according to the Lighthill, (1958) formulation. Results for pressure distributions, flow turning angles and aerodynamic coefficients have been compared to experimental data from NACA-65 airfoil cascades. A good agreement was observed. This methodology requires less computational time compared to the finite differences and finite element based models.

In the present work, a more complete model is presented aiming to specific application in cascades of axial turbomachinery. Modifications in the impenetrability condition caused by flow injection in the separation area, and viscous effects are introduced through transpiration technique (Ramirez et al, 2000, 1999). Once again panels technique by Hess and Smith (1967) is systematically reformulated in order to allow the flow velocity direction at the cascade inlet to be directly specified in magnitude, W1, and angle attack,β_1. Results are presented for cascades of NACA-65 profile for a range of angles attack, including the stall area. This work offers the designer a "direct design" tool with low computational cost. Another motivation is the possible extensions to "inverse design" methodology of axial turbomachinery blades regarding the presence of separation and viscosity.

Formulation of the Equations for the Flow in Linear Cascades

Linear cascades are planes rectified from cylindrical views of axial flow machinery. Fig. (1) shows a scheme of an infinite linear grid in the complex plane $z = x + \hat{i}y$, where x is the axial axis and $\hat{i}$ is the imaginary unity $\sqrt{-1}$.

The cascade is composed by identical profiles equally spaced with distance t, chord length l and stager angle β, the angle between blade chord and axial direction.

The study of the relative velocity field $\vec{W}$ in the cascade is desired, outside the profiles is desired. The assumptions of potential, incompressible, steady and bi-dimensional flow will be considered here. The flow parameters will be represented by the flow angles in the inlet and outlet β_1 and β_2, the deflection angle of the flow in the cascade, $\Delta\beta = (\beta_1 - \beta_2)$; and by velocities of the flow in the inlet and outlet $\vec{W}_1$.and $\vec{W}_2$

The velocity of the non-perturbed flow is given by the average of the vector velocities in the inlet and the outlet: $\vec{W}_\infty = (\vec{W}_1 + \vec{W}_2)/2$. The circulation on the profile is defined as $\Gamma_P = \oint W_{\tan} ds$ where $W_{\tan}$ is the outer tangential velocity at the profile boundary. Figure 1 shows the geometry of a linear cascade and the its velocities diagram.

Hess and Smith Panel Method in Cascades

Details of the basic formulation of the Hess and Smith (1967) panel method is depicted in the work of Petrucci (1998), in details. The airfoil is approximated by an inscribed polygon selected as to give a reasonable representation of the airfoil contour. The segments of polygons are denominated panels usually concentrating a larger quantity of these segments the region of the leading and trailing edges. Uniform distributions of sources and vortex are used; the

intensities of sources are the variables and the intensities of vortex are specified as a sinusoidal function that becomes zero at the trailing edge and reaches the maximum value γ_{max} in the leading edge, $\gamma_{(s)} = \gamma_{max} . F(s)$, Thus,

$$F(s) = \frac{1}{2}\left[1 + \sin\left[\pi\left(\frac{2 \cdot s}{s_l} - \frac{1}{2}\right)\right]\right] \quad (1)$$

In Eq (1), s represents the coordinate of the profile from the trailing edge where $s = 0$, going through the outer of the profile with the inlet at right and returning to the trailing edge $s = s_t$. This kind of distribution avoids the false aerodynamic loads in the area of the sharp trailing edge verified in the classical method of Hess and Smith, which uses a constant distribution of vortices in the whole profile, representing difficulties in the correct application of Kutta Condition. The modification of the basic formulation of Hess and Smith was tested successfully in various situations for profiles with sharper trailing edge, such as the case of the isolated profile of Joukowsky (Karamcheti, 1980) and the cascade of Gostelow in Petrucci's work, (1998).

The expression for the *conjugate complex* velocity in the point of control z_{ci} of panel i, induced by distribution of sources and vortex of all panels j, is given by:

$$\overline{W}(z_{c_i}) = \overline{W}_\infty + \sum_{j=1}^{N} \frac{g_j e^{-i\beta_j}}{2\pi} \log\left[\frac{\sinh(z_{c_i} - z_j)/t}{\sinh(z_{c_i} - z_{j+1})/t}\right], \quad (2)$$

where g_j represents the linear sources and vortex densities, $g_j = \sigma_j + \hat{i}\gamma_j$, t the blade pitch of cascade, β_i the panel angle i related to axis x and N the number of panels. Equation 2 can be separated in two parts, one referring to the sources and the other referring to the vortices. For $i = j$, it is necessary to consider the special; effect of self-induction.

For the given cascade geometry and the mean flow angle, Eq. (2) is applied to all points of control, resulting in a system of N linear algebraic equations for the N intensities of sources. The maximum intensity of vortex is determined by the application of the Kutta Condition.

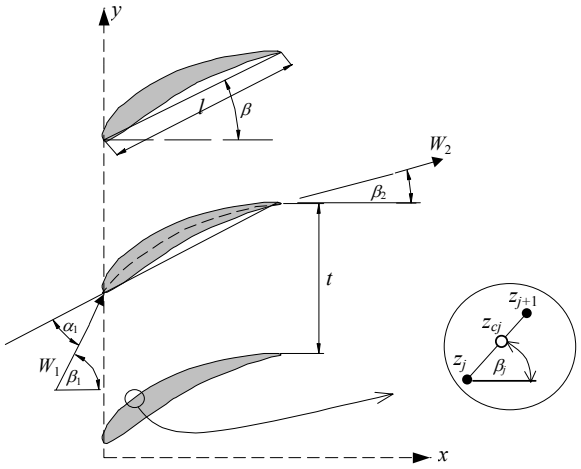

Figura 1a . Linear Cascade

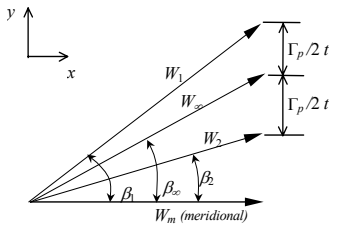

Figure 1b. Velocity diagram.

Reformulation of the Hess & Smith Method for a Given Inlet Angle.

It is important to notice that the numerical technique of Hess and Smith (1967) was first implemented to study the flow in isolated profiles for flight aerodynamics. In that technique the angle of attack α_∞, is measured relative to the chord of the profile, and the velocity $\vec{W}_\infty$ is used for the calculation of the distribution of singularities. For cascades of profiles in the situation of turbomachinery rotor, the inlet W_1 and the inlet angle, β_1, measured relative to the axial direction (Emery et al, 1957) are usually fixed. To obtain the angle β_1, in the first situation, different values of α_∞ must be tested iteratively, until a circulation is obtained around the airfoil compatible with velocities diagram (Fig.1). This process increases significantly the time of computation mainly when it is intended to make

viscous/non-viscous interactions. Consequently it is convenient to reformulate the method of Hess and Smith to give directly the cascade inlet angle and to perform the potential calculation straight, without iterations.

From triangles of Fig.1, a relationship can be obtained between the mean conjugate complex velocities $\overline{W}_\infty$ and the inlet $\overline{W}_1$, that is:

$$\overline{W}_\infty = \overline{W}_1 + \hat{i}\,\frac{\Gamma_{pa}}{2t} \ . \qquad (3)$$

Equation.(3) is substituted in to Eq.(2) and the components of the normal velocity W_n and tangential W_t to the profile boundary are then isolated:

$$W_{t_i} = \mathbf{Re}\left[\sum_{j=1}^{N}\frac{\sigma_j e^{-\hat{i}\beta_j}}{2\pi}\log(K)e^{\hat{i}\beta_i} + \gamma_{\max}\sum_{j=1}^{N}\hat{i}\,\frac{e^{\hat{i}\beta_j}}{2\pi}\log(K)\cdot e^{\hat{i}\beta_i}F_i + \left(\overline{W}_1 + \hat{i}\,\frac{\Gamma_{pa}}{2t}\right)e^{\hat{i}\beta_i}\right], \qquad (4)$$

$$W_{n_i} = \mathbf{-Im}\left[\sum_{j=1}^{N}\frac{\sigma_j e^{-\hat{i}\beta_j}}{2\pi}\log(K)e^{\hat{i}\beta_i} + \gamma_{\max}\sum_{j=1}^{N}\hat{i}\,\frac{e^{\hat{i}\beta_j}}{2\pi}\log(K)\cdot e^{\hat{i}\beta_i}F_i + \left(\overline{W}_1 + \hat{i}\,\frac{\Gamma_{pa}}{2t}\right)e^{\hat{i}\beta_i}\right], \qquad (5)$$

where K is the argument of the logarithmic function at Eq. (2).

The circulation around the blade is represented by a numerical integration which uses the function defined in Eq.(1).

$$\Gamma_{pa} = \gamma_{\max}\sum_{j=1}^{N}F_i\Delta s_i \ , \qquad \Delta s_i = \left\|z_{i+1} - z_i\right\| . \qquad (6)$$

Equation (6) is substituted into Eqs. (4) and (5). Expressions for the tangential and normal velocities in the control points in terms of the inlet velocity, with the adequate effect of the vortex distribution are then calculated, being this way, the equations (4) and (5) can be rewritten in matrix form:

$$\{W_t\} = [B]\{\sigma\} + \gamma_{\max}\{D\} + \{W^1_{tan}\}, \qquad (7)$$

$$\{W_n\} = [A]\{\sigma\} + \gamma_{\max}\{C\} + \{W^1_{nor}\} \ . \qquad (8)$$

The brackets {} represent column vectors Nx1 and the square brackets [ ] square matrices $N \times N$. [A] and [B] are the matrices of the normal and tangential influence coefficient, respectively, that depend only on the geometry of the airfoil, the blade pitch, the stagger angle, and the number of panels; {D} and {C} represent the vectors of the normal and tangential influence of vortex; $\{W^1{}_{tan}\}$ and $\{W^1{}_{nor}\}$ are the vectors of the normal and tangential components in the cascade inlet; $\{W_n\}$ is the vector of the normal velocity imposed at the boundary of the profile.

According to the method of Hess and Smith for the potential flow around the bodies, the variables $\gamma_{\max}$ (vortex) and σ (source) from Eqs. (7) and (8) are determined by the simultaneous application of the two conditions. The first is the boundary condition of the impenetrability that requires a null normal velocity over the body surface: $W_n = 0$; the second is the Kutta Condition that requires a flow that doesn't turn around the trailing edge. One way to impose this condition is to requires the tangential velocities on the control points over panels of the trailing edge to be the same, but in the opposite direction, that is, $W_{tn} = -W_{t1}$. The following chapter will treat the breakaway and the modifications of normal velocities of transpiration in the boundary condition as well as the Kutta's Condition.

Separated Wake Simulation

The boundary condition of the normal velocity W_n (Eq. 8) can be modified in order to simulate the wake breakaway through the fictitious flow injection. Hayashi and Endo (1977) obtained a semi-empirical relationship that quantifies the flow to be injected into the portion of separation flow. They use the tangential direction of the breakaway velocity W_s on the point s_u (upper) and s_l (lower), defined by the angles β_u and β_l respectively, as shown in Fig.2. The direction of the flow is given by the angle β^* in a random point on the profile surface

between the points s_u and s_l, and it is admitted that the normal component of the velocity vary in a linear way with the distance s along the surface.

Based on the experimental data, Hayashi and Endo (1977) defined a semi-empirical correlation was obtained between the non-dimensional flow intensity and the angles β_u and β_l, applicable to different kinds of aerodynamic bodies, Eq (9).

$$Q_E / l_{sp} W_s = 0.25 + 0.55 \cos\left(\frac{\beta_u + \beta_l}{2}\right) - 1.70\, sen\left(\frac{\beta_u - \beta_l}{2}\right) - 1.26 \cos\left(\frac{\beta_u + \beta_l}{2}\right) sen\left(\frac{\beta_u - \beta_l}{2}\right) \quad (9)$$

where Q_E is the flow to be injected, W_s is the velocity in the breakaway point and l_{sp}, β_u, β_l, are the profile geometric parameters as shown in Fig. 2. The correlation was established in order to produce an approximate constant pressure in the separated wake.

Effect of Attached Boundary Layer

The effect of the attached boundary layer will be treated by the technique of "*transpiration*" that consists of fluid injection in the external flow based on the boundary layer displacement thickness. This technique was proposed originally by Lighthill (1958). Represented by the following expression:

$$W_{nt} = \frac{d}{ds}(W_t \delta^*). \quad (10)$$

In the Eq.(10) W_t is the outlet tangential velocity distribution in the boundary layer, calculated by the potential model, $\delta^*(s)$ is the distribution of the displacement thickness obtained from the boundary layer calculation and s is the natural coordinate around the profile.

To determine the displacement thickness distribution δ^*, boundary layer momentum thickness θ, form factor $H = \delta^*/\theta$, superficial friction coefficient c_f and point of separation, the von Kármán equation of *momentum*, is solved numerically, given a known velocity distribution (which means to specify the pressure gradient). To solve this equation, the following methods and criterions are established: integral method of Thwaites for the area of laminar boundary layer; Michel's criterion for the transition between laminar and turbulent; and Head for the turbulent, boundary layer. The turbulent separation is defined by the form factor $H = 2{,}4$. The computational code for the calculation of the boundary layer was obtained from the work of Cebeci & Bradshaw (1977).

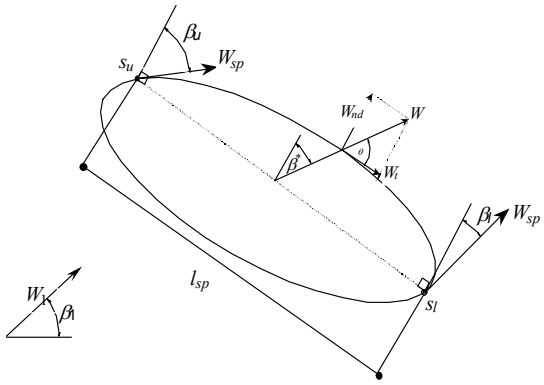

Figure 2. Definition of the normal velocity component, W_{nd}.

Extended Hess and Smith Method for Aerodynamic Profiles With and Without Separation

The proposed extension my be used at any portion of the attached boundary layer considering the corresponding viscous effects quantified through the transpiration technique. In the separation area the extension will have value only for profile suction side breakaway situations. In this area the theoretical injection flow Q_T is given by separated normal velocities (W_{nd}) and by the length ΔS of the outline distance with separation, assuming that the velocity W_{nd} raises linearly from zero at the separation point:

$$Q_T = \sum_{i=p_s}^{N} W_{nd_i} \Delta S_i / 2, \quad (11)$$

where: p_s is the index that represents the separation point (random beginning), ΔS is the length along the profile surface in the breakaway area, and N the number of panels.

Connecting appropriately Eqs. (9) and (11) and incorporating the transpiration velocities, one has:

$$\{W_n\} = \{K\}W_s + \{W_{nt}\}\ , \qquad \{K\} = \frac{2f(\beta_u, \beta_l)}{l_{sep}}\{S\}, \tag{12ab}$$

where W_s is the separation velocity and {S} is the local coordinate vector of the separation area from the separation point. In Eq. (12a) the first term of the right represents the normal injection velocity vector that is a function of the separation velocity W_s and of the geometrical parameters: β_u, β_l, I_{sep} and S_i. The second term, the transpiration velocity of the attached boundary layer, is the vector of normal velocity around the aerodynamical body W_n. It is possible to substitute the outline assumption of W_n (Eq. 12a) in Eq. (8), resulting in the following matrix equations:

$$\{K\}W_s + \{W_{nt}\} = [A]\{\sigma\} + \gamma_{\max}\{C\} + \{W^1_{nor}\}, \tag{13}$$

$$\{W_t\} = [B]\{\sigma\} + \gamma_{\max}\{D\} + \{W^1_{tan}\}. \tag{14}$$

Substituting the source intensity σ from Eq. (13) in Eq. (14):

$$\{W_t\} = \left(-[B][A]^{-1}\left(\{W^1_{nor}\} + \{W_{nt}\}\right) + \{W^1_{tan}\}\right) +$$

$$+\gamma_{\max}\left(-[B][A]^{-1}\{C\} + \{D\}\right) + W_s[B][A]^{-1}\{K\}. \tag{15}$$

Making all the matrix operations on the Eq.(18), it results:

$$\{W_t\} = \{VINF\} + \gamma_{\max}\{VGAMA\} + W_s\{VNOR\} \tag{16}$$

Note that in Eq. (16), vortex intensity γ_{max} and the velocity W_s are unknown which may be calculated by a change in the Kutta's condition, that is, the velocity at the separation point W_s will be the same as the velocity at the trailing edge in the lower side; $W_s = W_{ps} = -W_1$. From Eq. (19), it can be obtained the system of two equations with two variables W_s and γ_{max}, where the subscript 1 refers to the first panel of the trailing edge on the lower side and p_s to the panel where the separation point is fixed. Solving the system the values $\gamma_{\max}$ and W_s are obtained.

The value of the pressure coefficient, C_p, is calculated taking in to count the component of the normal and tangential velocities:

$$C_{p_1} = 1 - \left(\frac{W_{\tan}}{W_1}\right)^2 - \left(\frac{W_n}{W_1}\right)^2. \tag{17}$$

Algorithm for Calculation.

The methodology for calculating the flow with separation in aerodynamic bodies, including the viscous effects, is based on two computational codes 1) The potential code for calculating the flow in cascades, based on the numerical technique of Hess & Smith with modifications to simulate the effect of the separated wake; 2) The boundary layer code to determine the separation point and transpiration velocities. The computational codes will be quickly described as follows:

For the code 1, is supplied initially: cascade solidity $\lambda = l/t$, stagger angle β, inlet angle β_1, Reynolds number *Re*, number of panels *N,* and reference airfoil coordinates. An initial position for the separation point is also introduced, where a fictitious fluid injection is imposed. Initially the separation point must be fixed close to the trailing edge; the program, re-positions iteratively this point until reaches convergence with the separation point obtained through boundary layer calculation.

The modified potential flow calculation supplies new velocity distributions where the boundary layer code will be utilized to indicate the new separation point position at the airfoil suction side. The boundary layer code is utilized iteratively until convergence is achieved for the separation point fixed at the potential calculation. When 160 to 200 panels are used is verified a optimum convergence above the control point. However, for less panels it is necessary to consider as stop criterion the tolerance in the distance between the fixed point in the potential calculation and the one determinated by the boundary layer code.

After the region for injection was defined, a second iterative process is activated. Then the normal velocities of transpiration W_{nt} were introduced in the region where the flow was attached. The normal velocity components are then obtained from the Lighthill equation, Eq (10). The transpiration velocity values are sub-relaxed in each iteration with selected relaxation factors *FR*:

The distributions of the transpiration velocity along the blade and flow injection are calculated iteratively until satisfactory overall convergence is obtained. A means to check the convergence is the drag coefficient variation ($\left|C_{d\,ant} - C_{d\,atual}\right| \le 10^{-6}$).

The flow deflection angle in the cascade is calculated using the effective circulation and blade spacing of the cascade (Fig.1). The effective circulation is calculated by integral of tangential velocities around airfoil. In the region of separation the tangential velocity is obtained from separation velocity (constant) and normal velocity of flow injection, that is:

$$\Gamma_{ef} = \oint W_t ds \cong \sum_{i=1}^{N} W_{t_i} \Delta s_i \qquad (17)$$

$$W_t = \sqrt{\left| W_s{}^2 - W_n{}^2 \right|} \qquad (18)$$

Drag Coefficient.

Based on the works of Speidel (1954) and Schlichting (1959), the drag coefficient is defined as:

$$C^*_{d_1} = 2\,\theta_{bf}\,\frac{\cos^2\beta_1}{\cos^3\beta_2}\cos\beta_\infty\,, \qquad (19)$$

where θ_{bf} is the boundary layer momentum thickness at the trailing edge for the suction and pressure sides or the place where the boundary layer separation occurs, $\theta_{bf} = \theta_{bf\,(suction)} + \theta_{bf\,(pressure)}$.

Speidel (1954), from theory and experimental data, obtained one empirical correlation for determination of the additional boundary layer momentum thickness in the separation region, for suction side, θ_{sep}.

$$\theta_{sep} = \frac{1}{2} y_{tA}\left[\left(\frac{W_s}{W_2}\right) - 0{,}9\right] \qquad (20)$$

where: W_s is the separation velocity, calculated from Eq. (16), W_2 is the cascades outlet velocity and y_{tA} is half the profile thickness at the point of separation ($y_{(suction)A} + y_{(pressure)A} = y_{tA}$), (Sanger 1973).

The value of boundary layer momentum thickness in the separation region θ_{sep} can be added to Eq. (19), resulting the total drag coefficient:

$$C_{d_1} = 2\left(\theta_{bf} + \theta_{sep}\right)\frac{\cos^2\beta_1}{\cos^3\beta_2}\cos\beta_\infty \qquad (21)$$

For the drag calculation, the integration of drag and pressure coefficients, were not used, because lead to mistakes in the process of numerical integration. Such process depends strongly on the number of panel and kinematic parameters. In the case of cascades, the situation is much more serious, because drag force is defined by the mean velocity direction, which depends from the calculation. Therefore small mistakes in the determination of the direction of the velocity can introduce large errors in drag component, without substantially affecting the lift component that is dominant.

Pressure Drag Determination by Fluid Injection

It is possible to substitute the Speidel (19) formula with one more appropriate, based on the flow injection technique. A Kutta-Joukowski theorem extension has been proposed by Manzanares (2001) for bidimensional flow around any aerodynamic body when there is one region of fictitious flows. The classic solution for skin friction is not considered and only pressure drag will be considered in the separation region.

Manzanares (2001) proposed the following formulation to calculate pressure drag in the separated flow region:

$$C_{d_1(inj)} = \frac{2Q_E\left(W_s - W_\infty\right)}{W_1{}^2 l}, \qquad (22)$$

where, Q_E represents the flow injection, calculated from Hayashi correlation, W_s the

separation velocity calculated from the Eq. (22), W_∞ the vector-mean velocity (Fig. 2), W_1 the velocity of blade row , and l the blade chord.

Equation (30) requires that $W_s \geq W_\infty$. This constraint won't be satisfied for small angles attack when a small wake separation is used to guarantee the convergence. Therefore, situations where $W_s < W_\infty$ will be considered without physical meaning, resulting in $C_{d_1(inj)} = 0$.

To calculate the cascade drag, it is possible to add Eq. (22) to Speidel's Eq. (19) without considering the wake shear stress, resulting:

$$C_{d_1} = C^*_{d_1} + C_{d_1(inj)} \qquad (23)$$

Pressures Distribution and Cascade Deflection Exam-ples of Application

For the validation present methodology, the calculation results were compared with experimental data of Emery et al (1957) for airfoil in cascade NACA-(18)10. In this work, for each airfoil, three different stagger angles β and angles of attack α_1, are shown. Other situations of profiles can be found in Ramirez (2001). Figure (3) show the, results of the distributions of pressures for the indicate α, inlet flow angle β_1, ($\beta_1 = \beta + \alpha_1$) and cascade solidity λ parameters. The potential flow injection and transpiration models are presented. Compared with experimental data. For all cases 200, panels and Reynolds number of $2{,}54 \times 10^5$ were used. Agreement with as Emery et al (1957) data is achieved.

It must be emphasized that Emery et al (1957) data have an experimental error of ± 0,5º for the cascade angle of at design point deflection. This value may be higher at the "stall" region.

The case analyzed is the cascade NACA64-(18)10. Figure.3 shows the pressure distribution for small angle attack. Figure. 3d shows good agreement for angle attack $\alpha_1 \approx 20^o$, where are detected the maximum values of deflection. In this case the flow injection should be increased in a controlled way. Nevertheless, referencing to the methodology indicated in this work, empiric calibrations of the injection deserve other attention kind that will be explained as an open problem.

Lift and Drag Coefficients

Methodology validation also included, lift coefficient calculated by pressure and friction integration, and different calculations of drag coefficient, by Speidel (1954) correlation and by the flow injection formula.

The calculated points of aerodynamic coefficient (drag and lift) correspond to pressure distributions showed on Figures 3. The results are compared with Emery et al (1957) experimental data. The C_l/C_d maximum ratio is also shown because it defines the optimum condition of cascade performance, representing the maximum aerodynamic load with controlled drag forces.

The experimental drag measurement must be analyzed before they can be used for comparisons, because numerical values are relatively small and possibly large uncertainties due to measurement technique. The same must be applied to C_l/C_d ratio. More important here is the comparison of C_l/C_d relation with attack angle variations, and the possibility to find the optimum cascades with certain confidence, from C_l/C_d maximum relation.

The Fig. 4 shown the following results: lift coefficient C_l, drag coefficients $c_d^{(2)}$ (according Speidel) and the drag coefficient, obtained according to flow injection criteria $c_d^{(3)}$. In the upper portion of the figures, are the different values of $c_l/c_d^{(2)}$ e $c_l/c_d^{(3)}$ compared with experimental data (Emery et al 1957).

The lift values calculated from the potential model are shown, indicating the large differences of experimental data, as already expected.

Fig. 5a shows the aerodynamic coefficients for NACA65-(18)10 profile. Notice that the model can satisfactorily foresee stall for an angle attack around 20^o, corresponding to the maximum lift values. The drag curves, indicate notice that the calculated values (Speidel, 1954), $c_d^{(2)}$, and by flow injection, $c_d^{(3)}$, have similar behavior. However, the drag according to (Speidel), approaches experimental data on the region of lower of angles attack. The corresponding maximum values of $c_l/c_d^{(2)}$ and

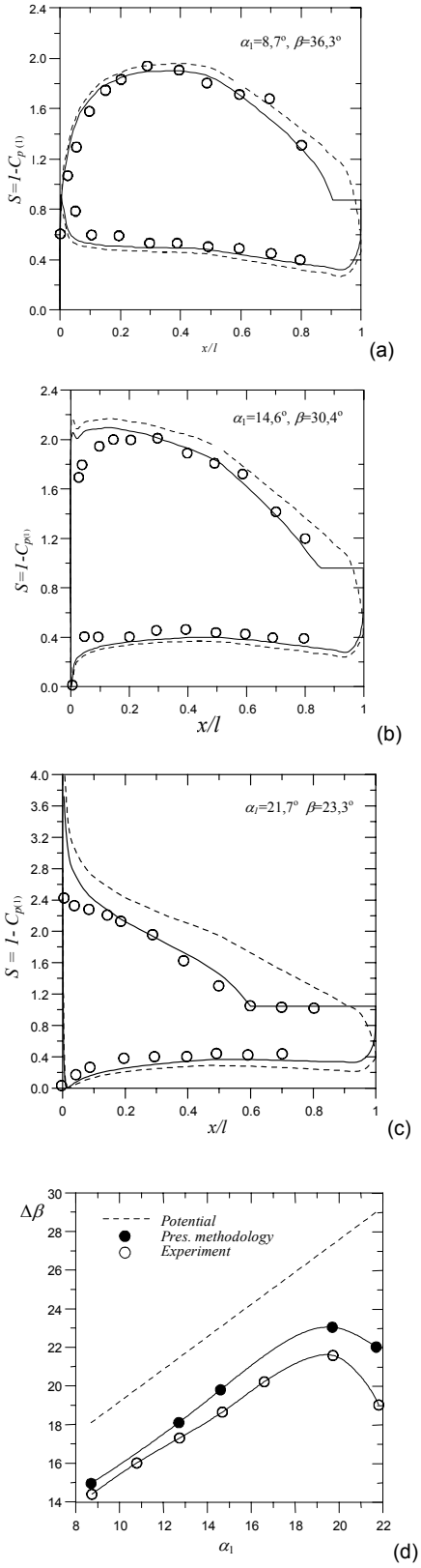

Figure 3. (a,b,c) Pressure distribution: ---- Potential, — Present Methodology, ○ Experiment
(d) Cascade deflection angle; NACA65-(18)10 airfoil , β_1=45°, λ =0,5 Re=3,54×10^5.

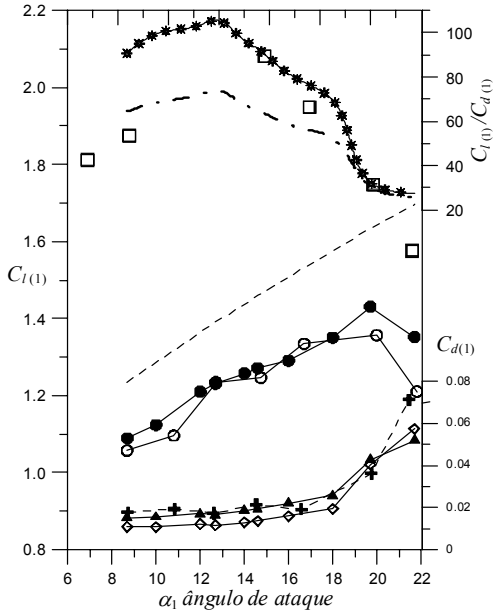

NACA65-(18)10, β_1=45°, λ=0,5

Figure 4.- Lift and drag coefficients: --- $C_{l\ (1)}$ potential, –○– $C_{l(1)}$ experimental, –●– Pres. methodology , --✚-- C_d experimental, –▲– $C_d^{(2)}$ (Speidel), –◇– $C_d^{(3)}$ (Inj. Flow),□ C_l / C_d experimental, –-–$C_l / C_d{}^{(2)}$, –✸–$C_l / C_d{}^{(3)}$.

$C_l / C_d^{(3)}$ occur practically at the same of angle attack. However, the values $C_l / C_d^{(2)}$ are closer to the experimental data.

Drag values calculated by the Speidel correlation and by flow *injection formula* approach experimental data on the lower range angles attack. For higher angles, the flow injection formula tends to underestimate the drag. When, the maximum values of $C_l / C_d^{(3)}$ relation tend to occur at angles nearer $C_l / C_d^{(2)}$ stall values.

The comparison between the procedures presented here, for the drag calculation is not conclusive yet and suggests the necessity of further systematic studies

Conclusions

The Hess & Smith (1967) method modified to simulate the flow in cascades, using the flow injection technique and transpiration velocities, produced satisfactory results for pressure distributions, cascade deflection angles, and lift coefficient. The results showed the strong influence of flow injection essentially near the

stall region. The inviscid-viscous interaction was proved to be efficient with the use of relaxation techniques on normal transpiration velocities. On the other hand, the methodology is more efficient with the use of Hess & Smith panel technique where the cascade inlet velocity is used directly, to determine singularities distributions.

The methodology for the calculation of cascade flow presented in this work is based on contour integration formulation, having as vantage the small computation cost in relation to the full Navier Stokes equations solution. This method can be physically more realistic, but have higher computation cost. The present model is a low cost tool for initial design of the turbomachine cascades.

References.

Cebeci, T., Bradshaw, P., 1977, "Momentum Transfer in Boundary Layers", McGraw-Hill/Hemisphere, Washington, D.C.

Emery, J.C., Herrig, L.J., Erwin, J. R., Felix, R., 1957, "Systematic Two- Dimensional Cascade Tests of Naca 65- Series Compressor Blades at Low Speeds", NACA TN 1368, pp-23

Gostelow,J,P., 1984, "Cascade Aerodynamics", Pergamon Press Ltd., New York

Hayashi, M., Endo, E., 1977, "Performance Calculation for Multi-Element Airfoil Sections with Separation", Trans. Japan Soc. Aero. Space Sci.,Vol 20, Nro 49.

Hess, J.L., Smith, A.M.O., 1967, "Calculation of potential Flow About Arbitrary Bodies", Progress in Aeronautical Sciences, Pergamon Press, vol. 8, pp. 1-138.

Lieblein S., 1959, "Loss and Stall Analysis of Compressor Cascades", Journal of Basic Engineering, pp 387- 400.

Lighthill, M.J., 1958, "On displacement Thickness", J.F1 Mech., 4, pp.383

Manzanares Filho, N., 1994, "Análise do Escoamento em Maquinas de Fluxo Axiais", Tese de Doutorado, ITA, São José dos Campos - Brasil.

Petrucci, R.D., 1998, "Problema Inverso do Escoamento em Torno de Perfis Aerodinâmicos Isolados e em Grades de Turbomáquinas", Tese de Mestrado, EFEI, Itajubá – MG, Brasil.

Ramirez, R.G., Manzanres, N.F., Petrucci, D.R., 2000, "Extensão do Método de Hess & Smith para Cálculo do Escoamento em Grades com Separação", Anais-CD, VIII Congresso Brasileiro de Ciências Térmicas, ENCIT 2000, Porto Alegre - Brasil.

Ramirez, R.G., Petrucci, D.R., Manzanares N.F., 1999, "Um Modelo de Escoamento Potencial para Cálculo da Distribuição de Pressões em Torno de Aerofólios com Separação Massiva", Anais IV Congreso Iberoamericano de Ingenieria Mecanica, CIDIM 99, Vol 3- Termofluidos, Santiago – Chile.

Ramirez R.G.C., 2001, "Análise do Escoamento em Grades de Turbomáquinas Axiais Incluindo o Efeito de Separação da Camada Limite" (In Portuguese), Tese Doutorado, Escola Federal de Engenharia de Itajubá, M.G

Sanger N. L., 1973, "Two- Dimensional Analytical and Experimental Performance Comparison for a Compressor Stator Section with D- Factor of 0.47", NASA Technical Note, TN D-7425, pp 1-38.Washington.

Spalart.,P.R., Allmaras, S.R., 1992, " A One-Equation Turbulence Model for Aerodynamics Flows", AIAA Paper 92-0439.